Microelectronic Engineering 88 (2011) 2946–2950

Contents lists available at ScienceDirect

Microelectronic Engineering

journal homepage: www.elsevier.com/locate/mee

Single-material-based multilayered nanostructures fabrication via reverse thermal nanoimprinting

S.Y. Yew, T.S. Kustandi, H.Y. Low, J.H. Teng, Y.J. Liu, Eunice S.P. Leong *

*Institute of Materials Research and Engineering, A*STAR (Agency for Science Technology and Research), 3 Research Link, Singapore 117602, Republic of Singapore*

ARTICLE INFO

Article history:
Received 4 November 2010
Received in revised form 11 February 2011
Accepted 7 April 2011
Available online 20 April 2011

Keywords:
Reverse nanoimprint
Multilayer
Nanostructure

ABSTRACT

We demonstrated a multilayered, residual-free nanostructure by stacking a one-dimensional grating in an orthogonal arrangement via reverse thermal nanoimprinting and reactive ion etching technique using a single material (PMMA). We found that a good pattern transfer with minimal residual layers was mainly determined by four important factors: the concentration of PMMA in toluene solution, the type of fluorosilane used on the mold surface, and the temperature and pressure used in reverse nanoimprinting. The first layer was reverse-nanoimprinted at the temperature of 150 °C, while the subsequent layers were achieved at the onset temperature of the glass transition of PMMA. Experimental results showed that the compression of the bottom layer was inevitable due to a change in mechanical property of the PMMA after repeated reverse nanoimprinting process.

1. Introduction

Multilayered structures are widely used in many applications including nano-photonics [1–3], micro-fluidics [4], biomedical and tissue engineering [5]. Various techniques such as two-photon absorption [1], colloidal and nanosphere method [2,3,6], photolithography [7], holography [8–11] and nanoimprinting [12–16] have been developed. As a general criteria for the patterning process, it is desired to have (1) reduced number of steps in multilayer patterning, (2) single material for ease of removal, (3) residual-free layers for infiltration of structure with other materials, and (4) large area patterning. Nanoimprinting, though it is still challenging to fabricate multilayered structures, stands out from the aforementioned techniques in terms of easy fabrication, large area patterning, mass production, and cost effectiveness [17–19].

In principle, multilayered nanostructures can be fabricated through layer-by-layer stacking using nanoimprinting technique. In particular, reverse nanoimprinting is preferred since it does not require a planarization layer and this will ease the fabrication process greatly. The materials used for nanoimprinting can be either UV or thermal curable resists. The advantage of UV curable resists is that it avoids undesired residual layer after imprints [12,13]. But it is usually hard to remove the cured structures if they are to be used as sacrificial templates. In contrast, thermal curable resists can be easily removed by organic solvents. The only concern is the temperature required for the pattern transfer of the polymer from the mold to the substrate as this usually occurs near the glass transition temperature, T_g, of the resist. This may cause the underlying layer to flow and deform the structure. This concern may be addressed by stacking the polymer layers using two molds with different silane treatment (i.e., different surface energy). The structures remained in the mold with higher surface energy and can be transferred to the substrate by applying a pressure at a temperature that is slightly below the T_g of the polymer [14]. Alternatively, Bao et al. demonstrated the stacking of three different polymers with a reduced T_g via reverse thermal nanoimprinting [15]. These approaches, however, are limited by the number of layers and the choice of different materials that can be stacked. For this reason, intense research effort has been expended to use a single material for multilayered structure fabrication. Nakajima et al. have proposed the thermo-differential process for multilayered structures fabrication where the temperature of the bottom substrate is kept below T_g while that of the top mold is kept above T_g [16]. However, this approach requires the alteration of the imprinter machine. Bonding of polymer layers has also been explored using a thin SU8 adhesive layer [20], PVA mold [21] and Al sacrificial layer [22]. These methods require additional fabrication steps and removal of the SU8 adhesive and Al sacrificial layers may not be compatible with the device integration process. Direct thermal bonding of PMMA near T_g has also been demonstrated by Park et al. [20]. Nevertheless, such a method will cause a residual layer during the nanoimprint process and cannot ensure a 100% transfer yield. More importantly, it is still ambiguous if further layers can be stacked.

Given the limitations of the above mentioned methods, it is highly desirable to find a more cost-effective and simpler method to achieve multilayered structures. In this work, we adopt the

* Corresponding author. Tel.: +65 6874 7114; fax: +65 6774 1042.
E-mail address: leonge@imre.a-star.edu.sg (E.S.P. Leong).

0167-9317/$ - see front matter © 2011 Elsevier B.V. All rights reserved.
doi:10.1016/j.mee.2011.04.028

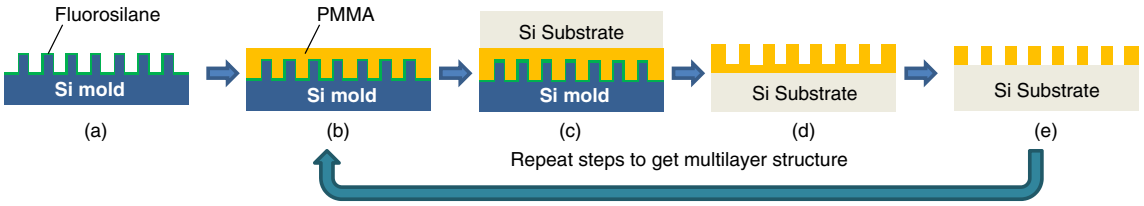

Fig. 1. Schematic diagram of the fabrication process for the multilayered nanostructures via reverse nanoimprinting: (a) overnight deposition of fluorosilane on silicon mold, (b) spin-coating of PMMA on fluorosilane-coated silicon mold, (c) reverse nanoimprinting process on silicon substrate, (d) removal of silicon mold from PMMA, and (e) removal of residual layer using reactive ion etching.

reverse thermal nanoimprinting technique and systematically studied and optimized the fabrication of a single-material, multilayered porous nanostructure over a large area. Our method allows direct orthogonal stacking of a one-dimensional grating at the onset temperature of the glass transition of the selected material. It overcomes two main limitations: (1) the tricky selection of different T_g materials; (2) the need for bonding and planarization layers. Hence, the process complexity is greatly reduced. In our experiments, PMMA is selected as the testing material. We demonstrate a three-layer porous PMMA nanostructure over $1 \times 1\ cm^2$ patterned area. The transfer yield is nearly 100%. Our method could be applied to other thermoplastic materials, such as polycarbonate or polystyrene. The multilayered porous nanostructures are potentially useful as sacrificial template for infiltration or scaffolds for bio-engineering.

2. Experimental

2.1. Nanofabrication

Fig. 1 shows the typical fabrication procedure for the multilayered nanostructures via reverse nanoimprinting. A $1 \times 2\ cm^2$ silicon mold (250 nm line and space gratings with ~200 nm depth) was cleaned in a piranha solution (a 3:1 mixture of 96% sulfuric acid and 30% hydrogen peroxide) at 120 °C for 30 min, rinsed with deionized water, dried in a stream of dry nitrogen, and finally put in a clean oven at 100 °C for 1 h. After that, the mold was exposed to oxygen plasma for 10 min in RIE Etcher, Sirus (Trion), operating at 200 mTorr oxygen pressure, 10 sccm oxygen flow rate, and 100 W electric power. The mold was further treated with a fluorosilane release agent through an overnight vapor deposition of either 1*H*,1*H*,2*H*,2*H*-perfluorodecyl-trichlorosilane (FDTS), phenethylmethyldichlorosilane (PEDS), or a mixture of FDTS and PEDS (Fig. 1(a)). To determine the surface energy of the silane treatments, the contact angles based on water and ethylene glycol for the bare Si substrates that undergo the same silane treatment are measured. The surface energies are then calculated using the formula given in Ref. [23].

In our experiment, the material used for reverse nanoimprinting was poly(methyl methacrylate) (PMMA), which has an average molecular weight of 120,000. PMMA was first dissolved into toluene solution at 3.7% concentration by weight and then spin-coated onto the fluorosilane-treated mold at 1500 rpm for 60 s (Fig. 1(b)). Next, the spin-coated mold was pre-baked at 90 °C for 5 min to remove the solvent. Reverse nanoimprinting was performed using the Obducat nanoimprinter (Sweden) by placing a piranha-cleaned silicon substrate on top of the PMMA-coated silicon mold. The mold was then heated to 150 °C and a pressure of 5 MPa was applied for 300 s to allow the transfer of PMMA from the mold to the substrate (Fig. 1(c)). The process ended by cooling the mold to 95 °C and releasing the pressure from the mold (Fig. 1(d)). The residual layer of PMMA material was removed through a brief reactive ion etching process in RIE Etcher (Plasmalab ICP 180, Oxford) operating at 65 mTorr oxygen pressure, 20 sccm oxygen flow rate, and 30 W electric power. The final product is then referred to as residual-free nanostructure. This process was repeated for subsequent stacking to obtain multilayered structures, with some modifications on the reverse-nanoimprint process condition.

2.2. Characterization

The morphologies of the multilayered structures were observed under a high-resolution scanning electron microscopy (SEM) (JEOL FESEM JSM-6700F). Temperature transition of PMMA was measured using a modulated differential scanning calorimeter (TA Instrument, DSC 2920 Modulated DSC).

3. Results and discussion

Fig. 2(a) shows the top and cross-sectional (inset) views of the first PMMA layer fabricated through reverse nanoimprinting. The key to a successful pattern transfer in reverse nanoimprinting lies

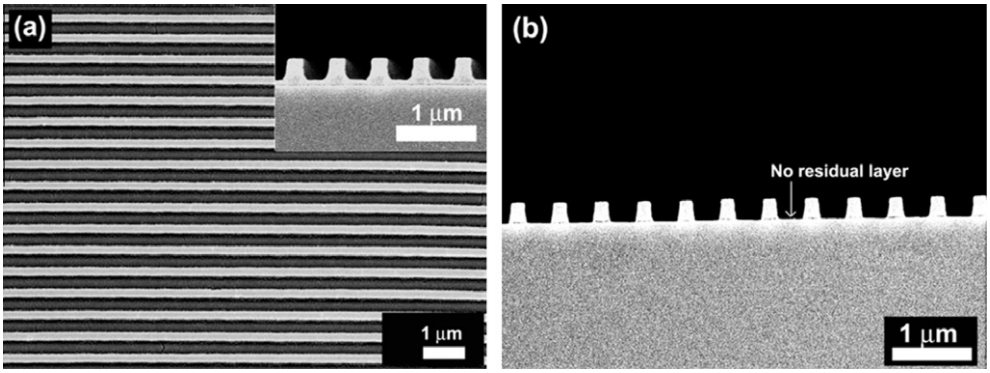

Fig. 2. SEM images of the first PMMA layer fabricated by reverse nanoimprinting (a) before and (b) after reactive ion etching. Inset of Fig. 2(a) shows the cross-sectional view of PMMA layer with ~80 nm thick residual layer.

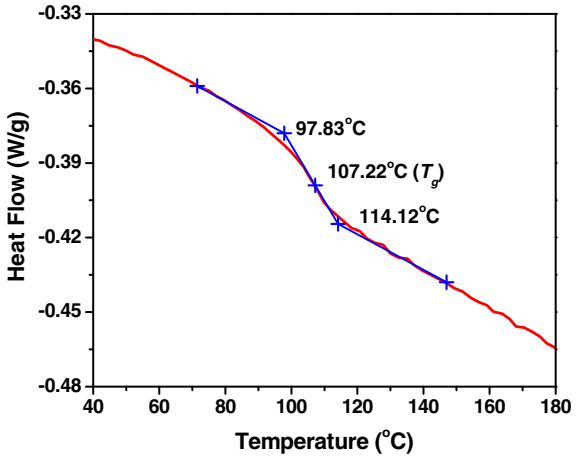

Fig. 3. DSC thermogram of PMMA (120,000 Mw).

in the fact that the substrate has to have a higher surface energy than the mold, hence allowing the polymer to have a stronger adhesion to the substrate and facilitating the detachment from the mold. We are able to demonstrate a large-area ($1 \times 2\ cm^2$) PMMA grating pattern on a silicon substrate. An array of ridges with ~250 nm width and ~200 nm depth was successfully replicated from the silicon master mold. We found that the type of fluorosilane used on the silicon mold and the concentration of PMMA in toluene solution are important so that PMMA can be released from the mold with minimal residual layer thickness. PEDS was used as an anti-adhesion release layer because it has a fairly low surface energy and allows for a uniform coating of PMMA on the mold. Here, the optimum concentration for PMMA in toluene solution was 3.7% by weight. Below that, a planar layer will not be formed on the mold and may cause incomplete filling of the trench regions of the surface relief patterns in the mold. At the optimum PMMA concentration, the residual layer had a minimal thickness of ~80 nm, as judged from the cross-section image. Before proceeding with the fabrication of the subsequent PMMA layers, a brief oxygen plasma etching of 100 s was found to be sufficient to completely remove the residual layer on the sample, as clearly shown in Fig. 2(b). A slight reduction of ~5% in the lateral dimension is found as a result of the etching process.

Stacking of the second layer PMMA nanostructures was performed by placing the mold orthogonally to the direction of the underlying layer. Because only a single material (PMMA) was used in our experiments, the reverse nanoimprinting conditions, such as temperature and pressure, have to be modified and re-optimized to maintain the structural integrity of the whole structures. Therefore, we have to understand the glass transition properties of our PMMA. Fig. 3 shows the temperature transition of PMMA used in our experiments. We can see that T_g is ~107 °C and the onset temperature of the glass transition is ~97 °C.

The second PMMA layer was first stacked at the T_g with a pressure of 6 MPa. Fig. 4(a) shows the cross-section of the two-layer PMMA nanostructures. It clearly shows that the underlying PMMA layer experienced significant compression of ~65% due to the softening and flowing of the first PMMA layer during the reverse nanoimprinting process. The thickness of the second layer was still 200 nm, while the thickness of the first layer was reduced to ~70 nm. This observation was further confirmed by examining the top view of the sample (Fig. 4(b)). It reveals that the ridges of the first PMMA layer were widened to ~350 nm and those of the second PMMA layer were maintained at ~250 nm in width.

To minimize the compression, an inventory strategy optimization was conducted to reverse-nanoimprint the second PMMA layer. Here, the compression is defined as the percentage in thickness difference in the first layer before and after the transfer of the second layer. Firstly, the second PMMA layer was reverse-nanoimprinted at different temperatures ranging from 97 to 105 °C at a fixed pressure of 3 MPa. Fig. 5(a) shows the measured compression as a function of the temperature. It is obvious that the compression of the first PMMA layer reduces at lower temperature. However, the temperature cannot go below 97 °C because the transfer yield obtained experimentally is below 70%. Nevertheless, we are able to achieve ~100% pattern transfer yield by conducting the reverse nanoimprinting at 97 °C, indicating a good adhesion between the first and second PMMA layers. This optimum temperature is also in excellent agreement with the DSC thermogram whereby PMMA started to flow at this temperature. It is noted, however, that a compression of ~37% was still observed on the first PMMA layer. This could be attributed to the change in the mechanical properties of the first PMMA layer. In the hierarchical structures demonstrated by Zhang et al., secondary and tertiary imprints of PMMA structures can be carried out subsequently at a temperature below the T_g of PMMA. This indicates that the modulus of the imprinted films is much smaller than that of the pristine films, thus allowing the secondary and tertiary imprints implemented at a low temperature [24,25]. Similarly in this study, when the second PMMA layer was reverse-nanoimprinted at below 97 °C, the first PMMA layer could have already started flowing. Although this seems to be sufficient for the two layers of PMMA to bond together, the adhesion is not strong enough to transfer the PMMA from the mold to the first layer grating. This is especially true since the PMMA layer on the mold was still in solid form and does not flow readily to

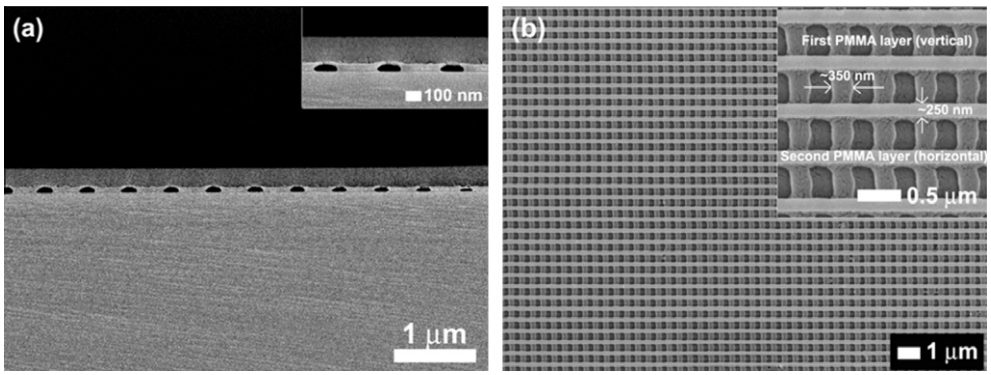

Fig. 4. SEM images of (a) cross-sectional view and (b) top view of double-layer PMMA nanostructures reverse-nanoimprinted at the T_g of PMMA (107 °C).

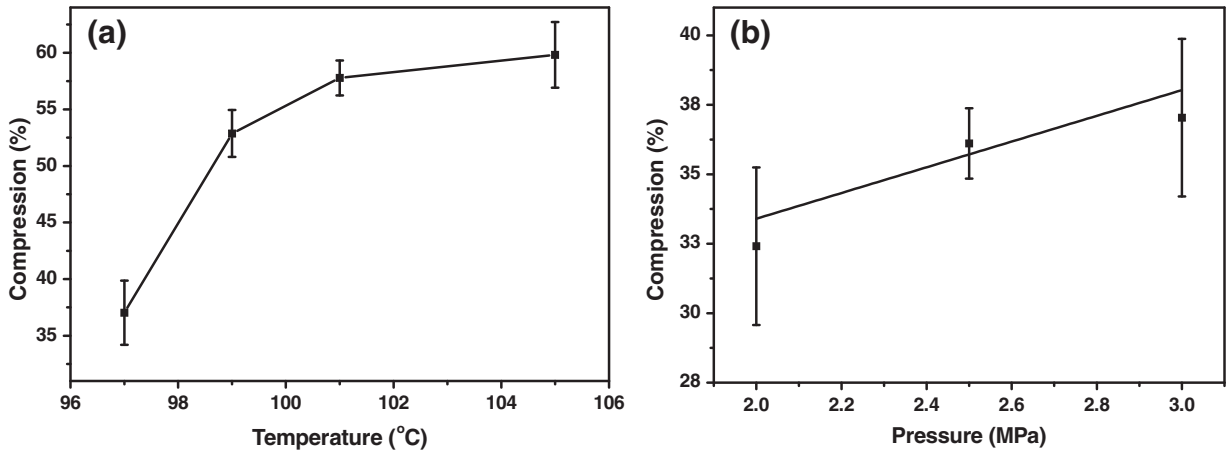

Fig. 5. Compression of the first PMMA layer at (a) different temperature with a pressure of 3 MPa and (b) different pressure with a temperature of 97 °C.

adhere to the underlying layer, hence resulting in a poor pattern transfer yield. On the other hand, at 97 °C, the polymer chain of the top layer starts to move and forms a better bond with the bottom layer. At the same time, the polymer chain of the bottom layer is also more mobile and becomes softer. This leads to compression when pressure is applied during the reverse nanoimprinting process.

Secondly, the compression was optimized by changing the pressure at the fixed temperature of 97 °C. The results in Fig. 5(b) show that the compression is linearly proportional to the applied pressure. When the pressure is below 2 MPa, a poor pattern transfer was obtained because the second PMMA layer could not adhere effectively to the first layer. Through this two-step optimization, we achieved the optimum temperature and pressure to conduct reverse nanoimprinting of the second and subsequent PMMA layers at 97 °C and 2 MPa, respectively.

Fig. 6 shows the top and cross-sectional views of the optimum double-layered structures. From Fig. 6(a), the compression of the first PMMA layer was dramatically decreased. The width of the grating was slightly widened to ~270 nm and the depth was ~140 nm (Fig. 6(b)). This corresponds to ~30% compression, as opposed to the 65% compression in the non-optimized process conditions.

It is worth pointing out that when reverse nanoimprinting is applied to transfer the second PMMA layer onto the underlying layer, PEDS cannot be used as an anti-adhesion release layer since the surface energy of the PEDS-treated silicon mold (~35.5 mJ/m^2) is very close to that of the PMMA material (~41 mJ/m^2) [26]. On the other hand, FDTS also cannot be adopted in reverse nanoimprinting because the surface energy is extremely low (~9.4 mJ/m^2), leading to a poor wettability of PMMA on the mold. The solution to this problem is to mix these two types of fluorosilanes at a ratio of 1:1 to obtain a sufficiently low surface energy (~17 mJ/m^2) on the mold. This not only

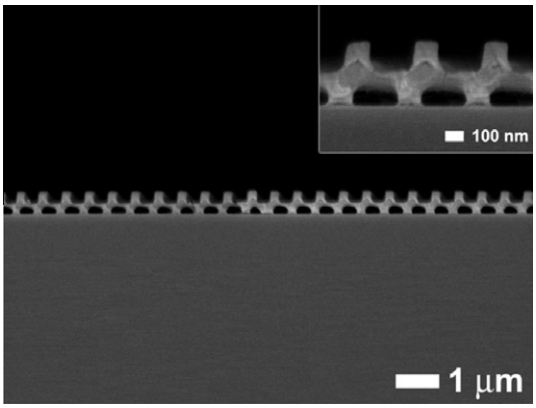

Fig. 7. SEM images of cross-sectional view of three-layer PMMA nanostructures fabricated by reverse nanoimprinting.

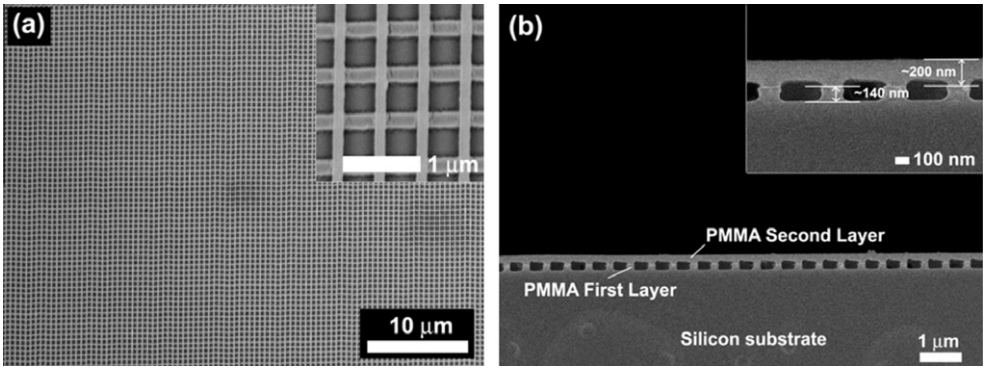

Fig. 6. SEM images of the (a) top view and (b) cross-sectional view of double-layer nanostructures. The temperature and pressure used to reverse-nanoimprint the second layer were 97 °C and 2 MPa, respectively.

allows excellent pattern transfer from the mold to the substrate but also maintains a uniform coating of PMMA on the mold with a variation of ±10 nm.

As a further step, a third PMMA layer was reverse-nanoimprinted onto the second layer. Fig. 7 shows the cross-sectional views of the achieved three-layer PMMA nanostructures using the optimized process conditions. The thickness of the first and second layers was reduced to ~130 nm (35%) and ~140 nm (30%), respectively, though they still fall within the range of compression charted in Fig. 5(b). The main challenge in stacking more layers using reverse nanoimprinting lies in the minimization of the compression at the bottom layers, which was affected by the changes of the modulus of PMMA and hence the tendency for it to flow more easily at lower temperature after many cycles of repeated reverse nanoimprinting process. Therefore, it would not be straightforward to fabricate more layers via reverse nanoimprinting using a single material. However, such technique could be combined with other methods but using the one-material reverse nanoimprinting as an intermediate step. For example, one could work with different thermoplastic polymers with different T_g and perform a three-layer imprint for each polymer.

4. Conclusions

We have demonstrated double-layer and three-layer residual-free PMMA nanostructures via reverse thermal nanoimprinting. This method enables the stacking of PMMA layers at the onset temperature of the glass transition and avoids the use of secondary materials for bonding as well as the need for planarization layer. A ~30% compression at the bottom layers is inevitable to ensure a good adhesion between the two PMMA layers (i.e., both layers have to flow to adhere well). By optimizing the reverse nanoimprinting parameters, it is possible to produce three-layer residual-free nanostructures using the PMMA material with minimal compression.

References

[1] J.F. Li, B.H. Jia, G.Y. Zhou, C. Bullen, J. Serbin, M. Gu, Adv. Mater. 19 (2007) 3276.
[2] J.S. King, D. Heineman, E. Graugnard, C.J. Summers, Appl. Surf. Sci. 244 (2005) 511.
[3] D.K. Hwang, H. Noh, H. Cao, R.P.H. Chang, Appl. Phys. Lett. 95 (2009) 091101.
[4] V. Vickerman, J. Blundo, S. Chung, R.D. Kamm, Lab Chip 8 (2008) 1468.
[5] I. Zein, D.W. Hutmacher, S.H. Teoh, K.C. Tan, Biomaterials 23 (2002) 1169.
[6] J.-H. Son, J. Wei, D. Cobden, G.Z. Cao, Y.N. Xia, Chem. Mater. 22 (2010) 3043.
[7] P. Yao, G.J. Schneider, D.W. Prather, E.D. Wetzel, D.J. O'Brien, Opt. Express 13 (2005) 2370.
[8] V. Mizeikis, K.K. Seet, S. Juodkazis, H. Misawa, Opt. Lett. 29 (2004) 2061.
[9] D.Y. Xia, J.Y. Zhang, X. He, S.R.J. Brueck, Appl. Phys. Lett. 93 (2008) 071105.
[10] M. Campbell, D.N. Sharp, M.T. Harrison, R.G. Denning, A.J. Tuberfield, Nature 404 (1999) 53.
[11] Y.J. Liu, X.W. Sun, Jpn. J. Appl. Phys. 46 (2007) 6634.
[12] C. Peng, S.W. Pang, J. Vac. Sci. Technol. B 24 (2006) 2968.
[13] N. Kehagias, V. Reboud, G. Chansin, M. Zelsmann, C. Jeppesen, F. Reuther, C. Schuster, M. Kubenz, G. Gruetzner, C.M. Sotomayor Torres, J. Vac. Sci. Technol. B 24 (2006) 3002.
[14] Y.P. Kong, H.Y. Low, S.W. Pang, A.F. Yee, J. Vac. Sci. Technol. B 22 (2004) 3251.
[15] L.R. Bao, X. Cheng, X.D. Huang, L.J. Guo, S.W. Pang, A.F. Yee, J. Vac. Sci. Technol. B 20 (2002) 2881.
[16] M. Nakajima, T. Yoshikawa, K. Sogo, Y. Hirai, Microelectron. Eng. 83 (2006) 876.
[17] C. Stuart, Y. Chen, ACS Nano 3 (2009) 2062.
[18] S.H. Lan, J.H. Song, M.G. Lee, J. Ni, N.K. Lee, H.J. Lee, Microelectron. Eng. 87 (2010) 2596.
[19] T.S. Kustandi, W.W. Loh, H. Gao, H.Y. Low, ACS Nano 4 (2010) 2561.
[20] H. Park, H.F. Li, X. Cheng, J. Vac. Sci. Technol. B 25 (2007) 2325.
[21] K.S. Han, S.H. Hong, H. Lee, Appl. Phys. Lett. 91 (2007) 123118.
[22] Y.N. Xu, W. Zhao, H.Y. Low, Microelctron. Eng. 83 (2006) 542.
[23] D.K. Owens, R.C. Wendt, J. Appl. Polym. Sci. 13 (1969) 1741.
[24] F.X. Zhang, H.Y. Low, Nanotechnology 17 (2006) 1884.
[25] F.X. Zhang, J. Chan, H.Y. Low, Appl. Surf. Sci. 254 (2008) 2975.
[26] <http://www.surface-tension.de/solid-surface-energy.htm>.